Radiotherapy and Oncology 132 (2019) 8–15

Contents lists available at ScienceDirect

Radiotherapy and Oncology

journal homepage: www.thegreenjournal.com

Original Article

1-[(4-Nitrophenyl)sulfonyl]-4-phenylpiperazine increases the number of Peyer's patch-associated regenerating crypts in the small intestines after radiation injury

Kruttika Bhat [a], Sara Duhachek-Muggy [a], Renuka Ramanathan [a], Mohammad Saki [a], Claudia Alli [a], Paul Medina [a], Robert Damoiseaux [b,c], Julian Whitelegge [b,d], William H. McBride [a,c], Dörthe Schaue [a,c], Erina Vlashi [a,c], Frank Pajonk [a,c,*]

[a] Department of Radiation Oncology, David Geffen School of Medicine, University of California at Los Angeles; [b] Molecular Screening Shared Resource, University of California at Los Angeles; [c] Jonsson Comprehensive Cancer Center at UCLA; and [d] Pasarow Mass Spectrometry Laboratory, University of California at Los Angeles, USA

ARTICLE INFO

Article history:
Received 25 April 2018
Received in revised form 20 November 2018
Accepted 21 November 2018
Available online 20 December 2018

Keywords:
Gastrointestinal acute radiation syndrome
Radiation mitigation
Intestinal stem cells
Peyer's patches

ABSTRACT

Objective: Exposure to lethal doses of radiation has severe effects on normal tissues. Exposed individuals experience a plethora of symptoms in different organ systems including the gastrointestinal (GI) tract, summarized as Acute Radiation Syndrome (ARS). There are currently no approved drugs for mitigating GI-ARS. A recent high-throughput screen performed at the UCLA Center for Medical Countermeasures against Radiation identified compounds containing sulfonylpiperazine groups with radiation mitigation properties to the hematopoietic system and the gut. Among these 1-[(4-Nitrophenyl)sulfonyl]-4-phenyl piperazine (Compound #5) efficiently mitigated gastrointestinal ARS. However, the mechanism of action and target cells of this drug is still unknown. In this study we examined if Compound #5 affects gut-associated lymphoid tissue (GALT) with its subepithelial domes called Peyer's patches.

Methods: C3H mice were irradiated with 0 or 12 Gy total body irradiation (TBI). A single dose of Compound #5 or solvent was administered subcutaneously 24 h later. 48 h after irradiation the mice were sacrificed, and the guts examined for changes in the number of visible Peyer's patches. In some experiments the mice received 4 daily injections of treatment and were sacrificed 96 h after TBI. For immune histochemistry gut tissues were fixed in formalin and embedded in paraffin blocks. Sections were stained with H&E, anti-Ki67 or a TUNEL assay to assess the number of regenerating crypts, mitotic and apoptotic indices. Cells isolated from Peyer's patches were subjected to immune profiling using flow cytometry.

Results: Compound #5 significantly increased the number of visible Peyer's patches when compared to its control in non-irradiated and irradiated mice. Additionally, assessment of total cells per Peyer's patch isolated from these mice demonstrated an overall increase in the total number of Peyer's patch cells per mouse in Compound #5-treated mice. In non-irradiated animals the number of $CD11b^{high}$ in Peyer's patches increased significantly. These Compound #5-driven increases did not coincide with a decrease in apoptosis or an increase in proliferation in the germinal centers inside Peyer's patches 24 h after drug treatment. A single dose of Compound #5 significantly increased the number of $CD45^{+}$ cells after 12 Gy TBI. Importantly, 96 h after 12 Gy TBI Compound #5 induced a significant rise in the number of visible Peyer's patches and the number of Peyer's patch-associated regenerating crypts.

Conclusion: In summary, our study provides evidence that Compound #5 leads to an influx of immune cells into GALT, thereby supporting crypt regeneration preferentially in the proximity of Peyer's patches.
 Radiotherapy and Oncology 132 (2019) 8–15

Exposure to ionizing radiation either from nuclear accidents, nuclear weapons or 'dirty bomb' attacks has severe effects on many normal tissue compartments. Survivors of the initial event experience a plethora of symptoms summarized under the term acute radiation syndrome or ARS. The gastro-intestinal ARS (GI ARS) is characterized by the rapid loss of the integrity of the epithelial layer lining the intestines. Subsequently, the resorption of nutrients and fluids in the gut is compromised and the intestine's barrier function lost, thus allowing pathogens to cross the epithelial layer and leading to sepsis. Sepsis, together with dehydration and

* Corresponding author at: Department of Radiation Oncology, David Geffen School of Medicine at UCLA, 10833 Le Conte Ave, Los Angeles, CA 90095-1714, USA.
E-mail address: pajonk@ucla.edu (F. Pajonk).

https://doi.org/10.1016/j.radonc.2018.11.011
0167-8140/

bleeding causes animals to die 7 to 10 days after radiation exposure. In mouse models of GI ARS the number of regenerating crypts per circumference 4 days after irradiation correlates with the radiation dose and determines if the animals recover [1].

Gut-Associated Lymphoid Tissue (GALT) is one of the largest lymphoid organs that line the small intestines, comprising up to 70% of body's immunocytes and acting as a barrier for invading pathogens in the gut. The domes of the aggregated lymphoid follicles are called Peyer's patches (PP). It has been previously reported that PP increase the radioresistance of adjoining crypts (PP crypts) compared to the non-patch-associated crypts (NP) [2]. In this study, PP crypts contained a greater number of clonogenic cells per crypt, the mitotic index for the whole PP crypt was significantly higher and PP crypt cell cycle time was lower than the NP crypts [2], all factors that promote radiation survival and regeneration of crypts.

Mass-casualty scenarios that involve radiation exposure come with multiple logistic challenges that make successful distribution of drugs to a large number of victims within the first 24 h after an incident unlikely. Currently, there are very few drugs known to mitigate the effects of radiation when applied 24 h after radiation exposure or later. A recent high-throughput screen performed by the UCLA Center for Medical Countermeasures against Radiation identified compounds with radiation mitigation properties to the hematopoietic system and the gut. Among these compounds 1-(4 -nitrobenzenesulfonyl)-4-penylpiperazine efficiently mitigated hematopoietic and gastrointestinal ARS [3,4]. For simplicity, we will be referring to our lead compound, 1-[(4-Nitrophenyl)sulfonyl]-4-phenylpiperazine as "compound #5". While compound #5 showed excellent efficacy *in vitro* and *in vivo* [3], both, the target cells and the molecular mechanisms of action for compound #5, have not been identified yet. In this study, we report that compound #5 increases the size and cellular content of PPs thereby increasing the number of PP-associated regenerating intestinal crypts.

Materials and methods

Animals

Lgr5-EGFP-IRES-creERT2 mice (heterozygous mice harboring a "knock-in" allele for EGFP driven by Lgr5 promoter) were purchased from the Jackson Laboratories (Bar Harbor, ME) and were bred with C57Bl/6 mice for maintaining the breeding colony. All the progeny from Lgr5-EGFP-IRES-creERT2 mice were genotyped by Transnetyx (Cordova, TN). Animals that were heterozygous for the EGFP transgene were used for. C3Hf/Sed//Kam, C57Bl/6 and Lgr5-EGFP-IRES-creERT2 mice were bred and maintained in a pathogen-free environment in the American Association of Laboratory Animal CARE-accredited Animal Facilities of Department of Radiation Oncology, University of California (Los Angeles, CA) in accordance with all local and national guidelines for the care of animals. The facility has a 12-h light-dark cycle (6am–6 pm). The animals were supplied Teklad 2020SX mouse diet and water ad libitum throughout all studies.

H&E staining

Longitudinal cross sections of C3Hf/Sed//Kam mouse small intestines were obtained and deparaffinization was performed by immersing the slides in 3 changes of xylenes for 2 min each. Slides were next rehydrated by immersing in 100%, 95% then 70% ethanol for 1 min each for 3 times. The slides were washed under running tap water and stained with hematoxylin for 8 min. After rinsing the slides under running tap water, the slides were dipped in acid alcohol 3 times, rinsed again, dipped in ammonia water 3 times, rinsed and dipped 30 times in 70% ethanol. They were then incubated with eosin for 3 min, and dehydrated by immersing in 95%, 100% ethanol and xylene for 1 minute each for 3 times.

Regenerating crypt assay

The regenerating crypt assay was performed as described by Withers and Elkind [5]. Briefly, PPs were identified by visual inspection and 5-mm-long segments adjacent or distant from the PPs were collected, fixed, and embedded in paraffin. 4-μm sections were stained with hematoxylin and eosin. Regenerating crypts were defined as basophilic cell clusters containing 10 or more cells, each with a prominent nucleus and little cytoplasm, lying close together and appearing crowded. The images were captured using a Keyence BZ 9000 fluorescence microscope (Itasca, IL) and the number of regenerating crypts per circumference was recorded.

Irradiation

Six- or twelve-week-old C3Hf/Sed//Kam mice were anaesthetized with an i.p. injection of 80 mg/kg Ketamine (Putney, NADA#200–073) and 4 mg/kg Xylazine (AnaSed, NADA# 139–236; Lloyd labs #4811) and whole-body irradiation was performed in groups of 2 mice using an experimental X-ray irradiator (Gulmay Medical Inc. Atlanta, GA) at a dose rate of 5.519 Gy/min for the time required to apply a prescribed dose. Control animals were sham-irradiated. The X-ray beam was operated at 300 kV and hardened using a 4 mm Be, a 3 mm Al, and a 1.5 mm Cu filter. NIST-traceable dosimetry was performed using a micro-ionization chamber and film dosimetry with films (Ashland Specialty Ingredients G. P., Bridgewater, NJ) placed at 5 positions inside the abdomen of mouse cadavers.

In vivo drug administration

Twenty-four hours after irradiation mice received a subcutaneous injection of 5 mg/kg of 1-[(4-Nitrophenyl)sulfonyl]-4-phenylpiperazine (Compound #5, Vitascreen, Champaign, IL) dissolved in 15 μl DMSO and then suspended in 1 ml of 1% Cremophor EL (Sigma–Aldrich, St. Louis, MO), in some experiments animals received daily injections for a total of 4 days. Control animals received DMSO/Cremophor EL only.

Immune cell isolation

Six-week-old C3Hf/Sed/Kam mice were sacrificed and approximately 10 cm of the small intestine was harvested and placed in a 10-cm dish containing ice-cold PBS + 1% Penicillin/Streptomycin (100 U/ml penicillin, 100 μg/ml streptomycin). The dish was then placed under a micro-dissection microscope to locate all the intestinal PPs in each mouse. PP domes were then dissected out of the intestines and finely chopped. Tissue suspensions were then poured into 4 mL of Spleen dissociation medium (Stem Cell Technologies, Vancouver, CA) and immune cells were isolated as per manufacturer's protocol. Briefly, the PP cells were incubated in the medium for 30 min at room temperature rocking horizontally. PP fragments were dissociated into a smooth suspension by gently squeezing each PP through a 70-μm mesh filter using the blunt end of a syringe. The immune cell suspension was then centrifuged at 300 × g for 10 min. The supernatant was discarded, and the cells were used for immune cell marker staining.

Immune cell marker staining

The immune cells isolated from PPs were subjected to staining with a panel of immune cell markers ((BD Biosciences, San Jose,

CA): CD11b–PE-Cy7 (Cat #561098), CD11c-APC-Cy7 (Cat #561241), B220-APC (Cat #561880), CD8-V450 (Cat #560471), CD4-PerCP-Cy5.5 (Cat #561115)) and CD45-PE (Cat #130-101-952, Miltenyi Biotech, Auburn, CA). The cells were blocked with Fc blocker (BD Biosciences) in 1% FBS in 1× PBS buffer on ice for 15 min and stained for different markers on ice for 20 min. The cells were washed with 1× PBS and analyzed for immune marker expression by flow cytometry CD45 expression was assessed using a MACSQuant Analyzer (Miltenyi Biotech). Multicolor immune cell markers profiles were acquired using a BD Biosciences Fortessa LSR machine. Data were analyzed using the FlowJo software package (10.4.2).

TUNEL assay

C3Hf/Sed//Kam mice either treated with Cremophor or Compound #5 were sacrificed 24 h after drug treatment, their intestines removed and fixed in formalin overnight. The tissues were embedded in paraffin and 4-μm sections were cut by the Translational Pathology Core Laboratory (TPCL) at UCLA. TUNEL assay was performed as per the manufacturer's protocol (TdT In Situ Apoptosis Detection Kit – Fluorescein, Cat #4812-30-K, Trivigen, Gaithersburg, MD). Deparaffinization was performed by warming the slides at 65 °C for 30 min. The slides were then immersed in 2 changes of xylenes for 5 min each. Slides were next immersed in 100%, 95% then 70% ethanol for 5 min each. This was followed by washes in 1X PBS, two times for 5 min each and then for 10 min at room temperature. Deparaffinized sections were treated with Proteinase K by placing 200 μL of the Proteinase K enzyme on the tissues and sealing it with a cover slip and incubating the tissues at 37 °C for 30 min. The slides were washed twice using deionized water for 2 min each. The slides were subsequently immersed in 1X TdT Labeling Buffer for 5 min, followed by 50 μL of labeling reaction containing TdT dNTP, TdT Labeling Buffer, 50X cobalt, and TdT Enzyme for test samples, minus the TdT enzyme for the negative control and plus the TACS-nuclease for the positive control sample and incubated at 37 °C for 1 h in a humidified chamber. The reaction was stopped using 1X TdT Stop Buffer for 5 min at room temperature. The slides were washed using 1X PBS twice for 5 min each. The samples were next covered with 50 μL of Strep-Fluor solution and incubated at room temperature for 20 min in the dark, washed and counter stained with Hoechst stain (10 μg/mL) for 3 min. After three additional washes the slides were mounted using Fluoromount (Sigma–Aldrich). The images were captured using a Keyence BZ 9000 fluorescence microscope.

Ki67 staining

Six-week-old C3Hf/Sed//Kam mice were sacrificed and approximately 10 cm of the small intestine was harvested and placed under a micro-dissection microscope to locate all the intestinal PPs in each mouse. Intestinal sections with PPs were grossed, fixed in formalin for 24 h and paraffin embedded. Longitudinal cross sections of the mouse small intestines from these blocks were obtained and deparaffinization was performed by warming the slides at 65 °C for 30 min. The slides were then immersed in 2 changes of xylenes for 5 min each. Slides were next immersed in 100%, 95% then 70% ethanol for 5 min each. The slides were washed under running tap water and then incubated in a 3% hydrogen peroxide/methanol solution for 10 min. The slides were rinsed with distilled water and incubated for 25 min in Citrate Buffer pH6 at 95 °C using Decloaking Chamber NxGen (Cat #DC2012, Biocare Medical, Pacheco, CA). The slides were then brought to room temperature, rinsed in PBST (Phosphate-Buffered Saline containing 0.05% Tween-20), and then incubated with an anti-mouse Ki67 antibody (1:100, Cat #12202, Cell Signaling, Danvers, MA) at room temperature for 1 h. The slides were rinsed with PBST and incubated with Dako EnVision + System–HRP-labeled Polymer Anti-Rabbit (Cat K4003, Dako, Santa Clara, CA) at room temperature for 30 min. After a rinse with PBST, the slides were incubated with DAB (3,3′-Diaminobenzidine) for visualization. Subsequently the slides were washed in tap water, counterstained with Harris' Hematoxylin, dehydrated in ethanol, and mounted with media.

Quantitative reverse transcription–PCR

Total RNA was isolated using TRIZOL Reagent (Invitrogen). cDNA synthesis was carried out using the SuperScript Reverse Transcription IV (Invitrogen). Quantitative PCR was performed in the My iQ thermal cycler (Bio-Rad, Hercules, CA) using the 2× iQ SYBR Green Supermix (Bio-Rad). C_t for each gene was determined after normalization to RPLP0 and $\Delta\Delta C_t$ was calculated relative to the designated reference sample. Gene expression values were then set equal to $2^{-\Delta\Delta Ct}$ as described by the manufacturer of the kit (Applied Biosystems). The PCR primers were synthesized by Invitrogen and designed for the mouse sequences of LPS binding protein (LBP) and RPLPO. Nucleotide sequences for the primers were as follows: LBP Forward 5′ GACCTGGACTTGACTCCGTC 3′; LBP Reverse 5′ AGGGTTTCAGCTTGGGATGTTGT 3′; RPLPO Forward 5′ GGCGACCTGGAAGTCCAACT 3′; RPLPO Reverse 5′ CCATCAGCACCACAGCCTTC 3′.

Lipopolysaccharide ELISA

For LPS ELISA assays, blood was collected on days 4, 5 and 8 after irradiation using EDTA as anticoagulant. Blood samples were centrifuged for 15 min at 1000 × g and aliquots were stored at −80 °C. The ELISA assay was performed using a kit (MyBiosource, San Diego, CA; catalog number MBS452438) following the manufacturer's instructions. Absorbance was read at 450 nm on a SpectraMax M5 plate reader (Molecular Devices, San Jose, CA). LPS concentrations were calculated against an LPS standard curve in GraphPad Prism version 6 (GraphPad Software, La Jolla, CA).

Enteroid in-vitro culture

Twelve-week-old female Lgr5-EGFP-IRES-creERT2 mice were randomly assigned to 4 groups and treated with 12-Gy TBI. Twenty-four hours later, the animals were treated with 4 daily treatments of compound #5 or solvent. On day 5, the animals were euthanized and the small intestine was harvested and placed in a 10-cm dish containing ice-cold PBS + 1% Pen/Strep (100 U/ml penicillin, 100 μg/ml streptomycin). The intestines were flushed with PBS and opened longitudinally. The villi were then gently scraped off using an ice-cold glass slide and washed with PBS three times. The intestines were chopped into small segments, dropped in a 50-ml tube containing 20 ml of ice-cold PBS with Pen/Strep and washed by pipetting up and down three times using a 10-ml pipette. The segments were then allowed to settle by gravity. The supernatant was discarded and the procedure was repeated approximately 15–20 more times until the solution was clear. The intestinal segments were re-suspended in PBS with 5 mM EDTA and rocked at 20 rpm for 15 min at room temperature. The segments were then allowed to settle by gravity and the supernatant was discarded. The segments were re-suspended in 10 ml of ice-cold PBS with 0.1% BSA, pipetted three times and allowed to settle. The supernatant was collected, and passed through a 70-μm filter into a 50-ml tube. This process was repeated 4 times and the supernatant were centrifuged at 290 × g for 5 min at 4 °C. The supernatant was discarded and the pellet was re-suspended in 10 ml of PBS + 0.1% BSA. The suspension was centrifuged at 200 × g

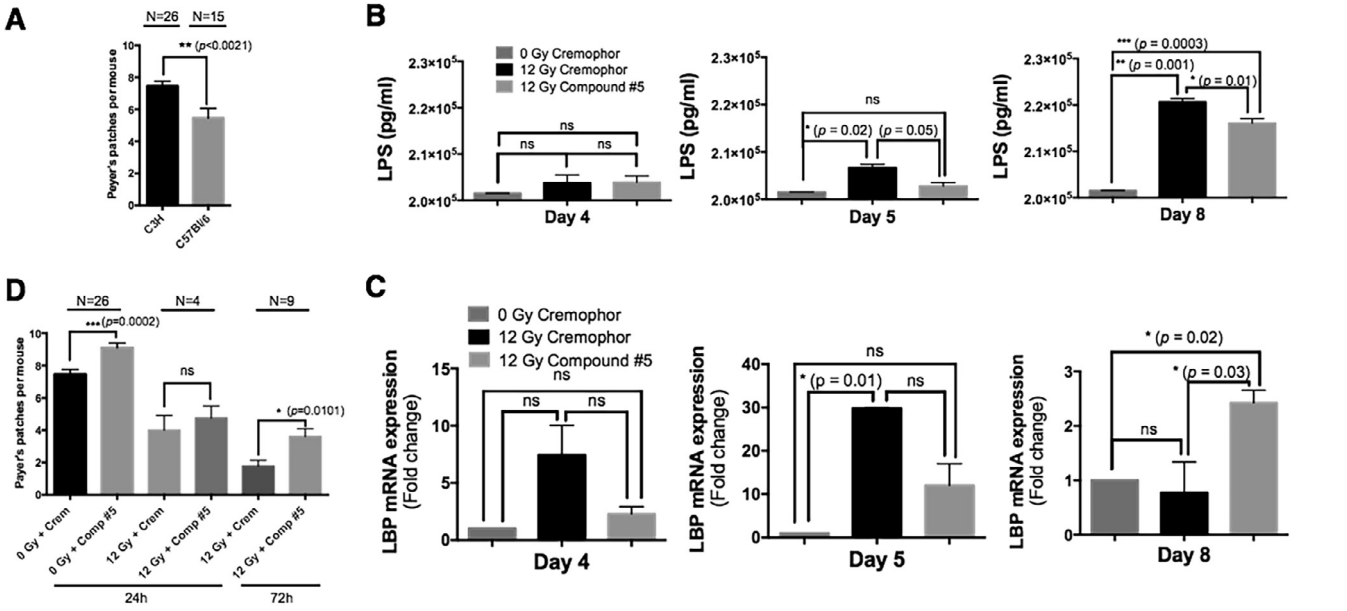

Fig. 1. Compound #5 increases the number of visible Peyer's patches in non-irradiated mice. Wild-Type C3H and C57Bl/6 mice were sacrificed, intestines were removed and the visible Peyer's Patches were counted. (A) C3H mice had significantly higher number of Peyer's Patches when compared to C57Bl/6 strain mice. (B) Plasma LPS levels in C3H mice on days 4, 5 and 8 after 12 Gy total body irradiation. On day 5, 12 Gy/Cremophor-treated animals show a significant increase in plasma LPS levels ($p = 0.02$, one-way ANOVA) while LPS levels in the plasma of 12 Gy/Compound #5-treated animals are not significantly elevated. On day 8 both, 12 Gy/Cremophor- and 12 Gy/Compound #5-treated animals show elevated plasma LMPS levels but the increase in 12 Gy/Compound #5-treated animals is significantly lower ($p = 0.01$, one-way ANOVA). (C) LBP mRNA expression in liver tissue of mice on days 4, 5 and 8 after 12 Gy total body irradiation. On day 5, 12 Gy/Cremophor-treated animals show a significant increase in liver LBP mRNA levels ($p = 0.01$, one-way ANOVA) while LBP mRNA levels in the livers of 12 Gy/Compound #5-treated animals are not significantly elevated. On day 8, LBP levels in the liver of 12 Gy/Compound #5-treated animals returned to baseline levels while LBP mRNA levels in the livers of 12 Gy/Compound #5-treated animals were significantly increase ($p = 0.02$, one-way ANOVA). C3H mice received 12 Gy of total body irradiation or sham irradiation, and 24 h later were administered with compound #5 (5 mg/kg) or Cremophor sub-cutaneously with a single dose for 24 h time point (48 h after irradiation) or with 4 daily injections for 72-h time point (96 h after irradiation). (D) Mice were sacrificed 24 h and 72 h after administering Compound #5, the small intestines were removed, and the visible Peyer's patches were counted. Compound #5 significantly increased the number of visible Peyer's patches in non-irradiated mice with only a single treatment of Compound #5. Mice irradiated with 12 Gy and treated with 4 daily injections of Compound #5 also significantly increased the number of visible Peyer's patches.

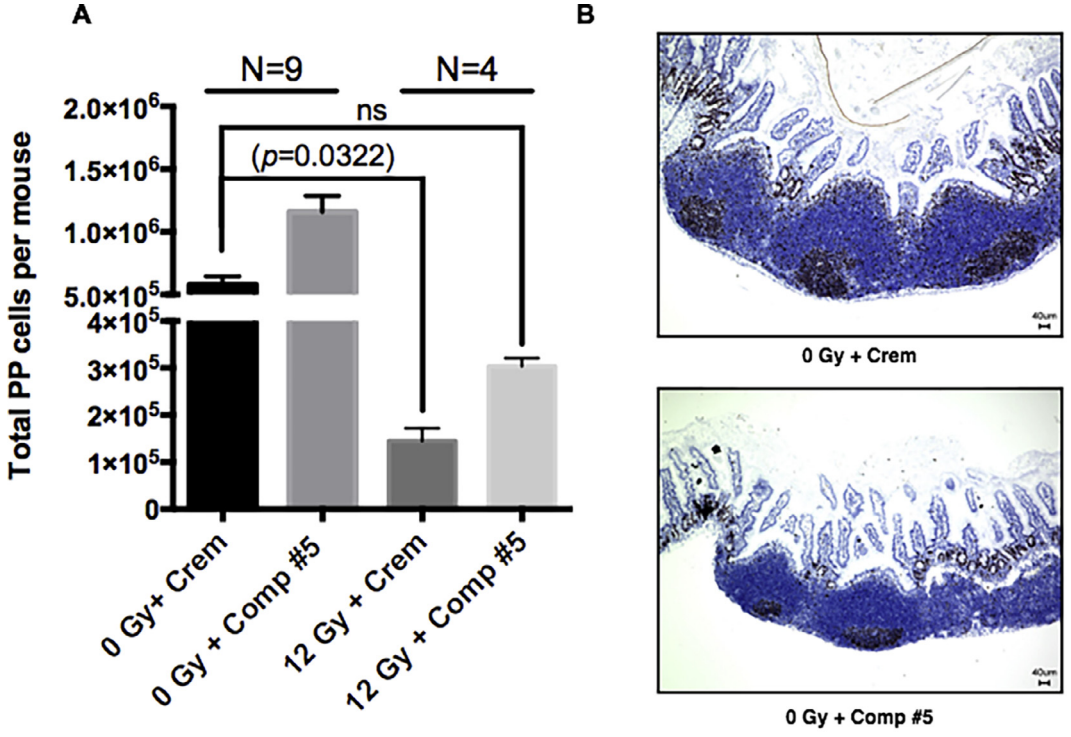

Fig. 2. Compound #5 increases the cells of Peyer's patches in both irradiated and non-irradiated mice. (A) C3H mice received 12 Gy of total body irradiation. Control animals were sham-irradiated. 24 h later animals received a single dose of compound #5 (5 mg/kg) or Cremophor subcutaneously. Mice were sacrificed 24 h after drug treatments (48 h after irradiation), the small intestines were removed, number of visible Peyer's patches were counted for each mouse and the cells of Peyer's patches were isolated to analyze the effect of compound #5 on Peyer's patch cell expansion. A single dose of 12 Gy significantly reduced the total number of Peyer's patch cells per mouse ($p = 0.0322$, one-way ANOVA). Treatment with compound #5 mitigated this effect of radiation. (B) Representative images of Ki67 stained Germinal Centers of Peyer's patches in 24-h Cremophor or compound #5-treated mice. Compound #5 did not increase the number of PP cells by increasing proliferation.

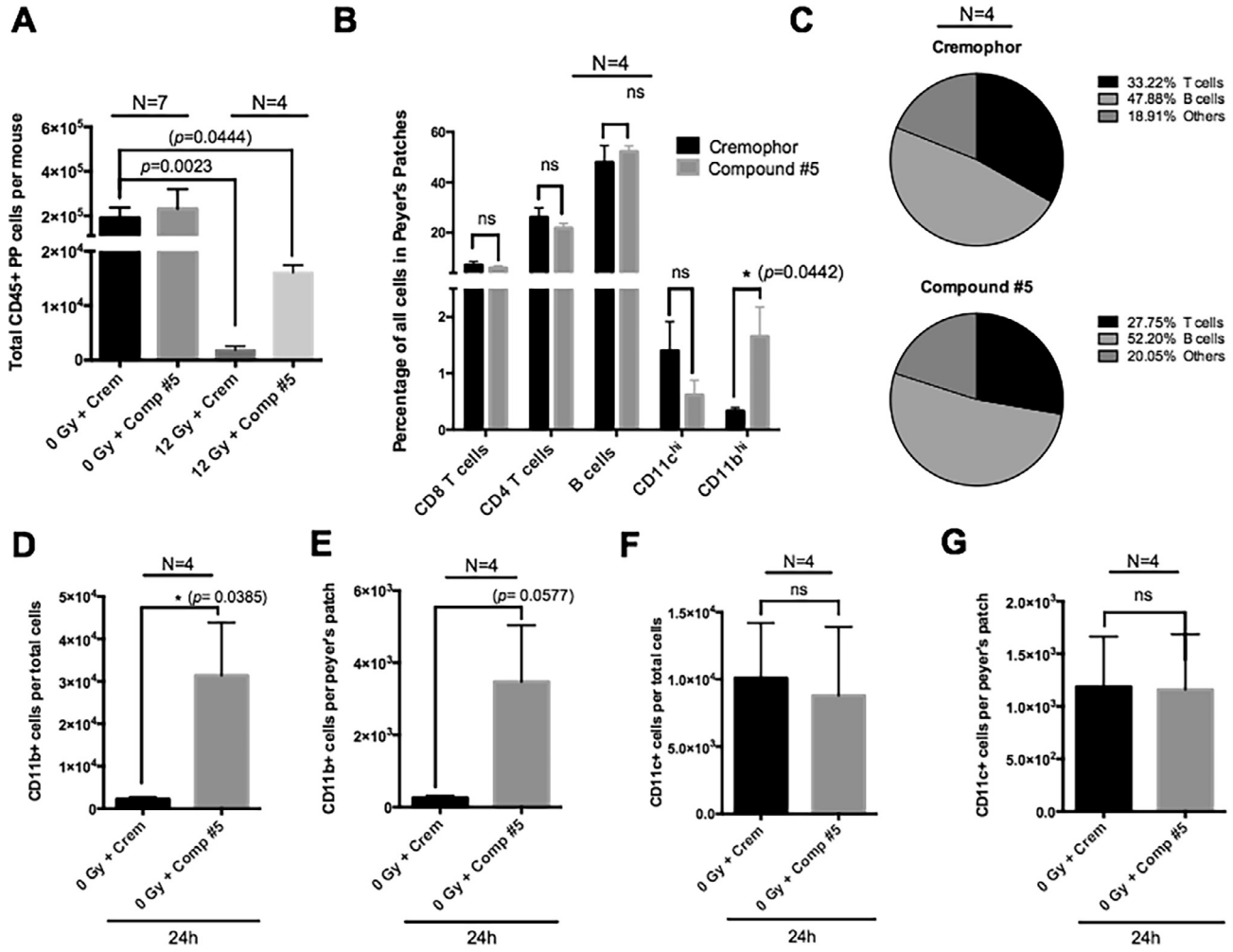

Fig. 3. Compound #5 increases the myeloid dendritic cell population in Peyer's patches. C3H mice received 12 Gy of total body irradiation or sham irradiation, and 24 h later were administered with a single dose of compound #5 (5 mg/kg) or Cremophor sub-cutaneously. Mice were sacrificed 24 hrs after administering compound #5 (48 hrs after irradiation), the small intestines were removed, and Peyer's Patch immune cells were isolated and subjected to immune cell profiling. The cells were stained with CD45-PE and flow cytometry was performed to gate for the $CD45^+$ cells. The percentage of $CD45^+$ cells obtained from each mouse was then calibrated to its total number of cells and the absolute number obtained was divided by the number of visible Peyer's patches. The results were expressed as total $CD45^+$ cells per mouse (A). A single dose of Compound #5 also significantly increased the percentage of $CD11b^{high}$ cells when compared to the Cremophor-treated mice (B). Pie charts depicting the distribution of T cells, B cells and other cells such as myeloid cells, dendritic cells, macrophages in Peyer's patches after single dose treatment of Compound #5 or Cremophor (C). The results from the effect of compound #5 specifically on $CD11b^{high}$ and $CD11c^{high}$ cells (C–E) were expressed as total $CD11b^{high}$ or $CD11c^{high}$ cells per mouse (D and E) or per Peyer's patch (F and G). Compound #5 significantly increased the absolute number of $CD11b^{high}$ cells but had no effect on $CD11c^{high}$ cells.

at 4 °C. The pellet was re-suspended in 5 ml of DMEM/F12 medium (Gibco). The number of crypts were determined by placing 10 μl of the crypt suspension on a glass slide and observing under the microscope. The crypt suspension was pelleted and resuspended in 50% complete IntestiCult Organoid Growth Medium (STEMCELL Technologies, Vancouver, BC) and 50% Matrigel (Corning, Corning, NY) for budding crypt assays or dissociated into single cells and analyzed by flow cytometry for the number of Lgr5-$EGFP^+$ cells.

Quantitative budding crypt assay

Budding crypt assays were conducted by plating 60 μl of crypt mixture, containing 15 crypts from each sample into each well of a pre-warmed 24-well plate. The Matrigel was allowed to solidify and then complete IntestiCult Organoid media was slowly added to cover the embedded enteroids. The media was changed daily for 6–8 days. The number of enteroids with budding crypts was determined once the crypts reached maturity on Day 6, and the percent of budding enteroids was calculated.

Statistics

All statistical analyses were performed using the Graphpad Prism software package. Unless stated otherwise, results were derived from at least three animals per group. A *p*-value equal to or smaller than 0.05 in Student's *t*-test or ANOVA test for multiple comparisons was considered statistically significant.

Results

Compound #5 increases the number of visible Peyer's patches

Inbred mouse strains are known for the differences in their response to ionizing radiation. Two of the most common mouse strains, C57BL/6 and C3H, react to irradiation distinctly differently in different organ systems and C57BL/6 mice are known for higher $LD_{70/30}$ (70% of the mice die by day 30) radiation doses after total body irradiation [4,6]. Yet, C3H mice are more resistant to total abdominal irradiation with an $LD_{70/10}$ dose of 20.5 Gy [4,7]. When we performed necropsies of untreated C3H and C57BL/6 control animals we noticed a significant difference in the number and size

of PPs in the small intestines of the two strains (C3H: 7.462 ± 0.30 C57BL/6 5.467 ± 0.6 patches/per mouse; $p < 0.0021$, Student's t-test), which was in agreement with the published differences in $LD_{70/10}$ radiation doses after total abdominal irradiation and the radioprotective function of PPs (Fig. 1A). We recently reported that compound #5 mitigates hematopoietic and gastro-intestinal ARS [3] but the underlying mechanism and target cells are unknown. Using an ELISA for LPS we observed increasing plasma LPS levels in animals treated with Cremophor. Plasma LPS levels in compound #5-treated animals also increased but on day 8 after irradiation when control animals reached the study endpoint LPS plasma levels in compound #5-treated animals were significantly lower than in control animals, thus indicating that compound #5 preserved the barrier function of the gut (Fig. 1B). This was further supported by significantly increased LBP mRNA expression in liver tissue of compound #5-treated animals extracted on day 8 after irradiation (Fig. 1C). In search for the target cells for compound #5 we hypothesized that radiation mitigation by this drug is mediated through an expansion of the gut-associated lymphoid tissues.

When C3H mice were treated with a single dose of compound #5 (5 mg/kg s.c., 24 h after irradiation) to mitigate gastrointestinal ARS after total abdominal irradiation we noticed a consistent and significant increase in the number of visible Peyer's patches in compound #5-treated animals. Even in sham-irradiated control animals the treatment with compound #5 increased the number of PPs from 7.462 ± 0.30 to 9.115 ± 0.27 patches/per mouse ($p = 0.0002$, Student's *t*-test) as early as 24 h after drug treatment (Fig. 1D). Not surprisingly, in animals irradiated with 12 Gy, 24 h after drug treatment and 48 h after irradiation, the number of visible PPs was decreased. At 72 h after drug treatment (96 h after irradiation) the number of visible PPs was decreased compared to sham-irradiated animals (7.46 vs. 1.778, $p < 0.0001$, Student's t-test) but treatment with compound #5 significantly increased the number of PPs from 1.778 ± 0.36 in Cremophor-treated animals to 3.6 ± 0.5 ($p = 0.0101$, Student's t-test) (Fig. 1D). Analysis of the total number of Peyer's patch cells/per mouse revealed a significant decrease in animals treated with a single dose of 12 Gy and Cremophor (Fig. 2A, $p = 0.0322$, one-way ANOVA). Treatment with compound #5 partially mitigated this effect of radiation and while the total number of PP cells per mouse was still reduced, the decrease was not significant (Fig. 2A, $p = 0.3261$, one-way ANOVA).

Next, we tested if the increase in cellularity resulted from decreased cell death or an increase in proliferation. In sham-irradiated animals both, control animals and compound #5-treated mice, showed only very few TUNEL-positive cells within the PPs, thus excluding inhibition of apoptosis as a mechanism for the observed increase in the total number of cells per PP (Supplementary Fig. 1).

Supplementary data associated with this article can be found, in the online version, at https://doi.org/10.1016/j.radonc.2018.11.011.

In order to test if the increase in cellularity was caused by compound #5-induced proliferation, intestinal sections of compound #5- or Cremophor-treated animals were stained for Ki67 24 h after drug treatment. Ki67-positive cells were found in the crypt regions and in the germinal centers of Peyer's patches with no obvious difference between the two treatment groups (Fig. 2B). Together these findings suggested that the observed increase in the total number of cells in PPs resulted from a recruitment of cells from other organs into the gut-associated lymphoid tissues.

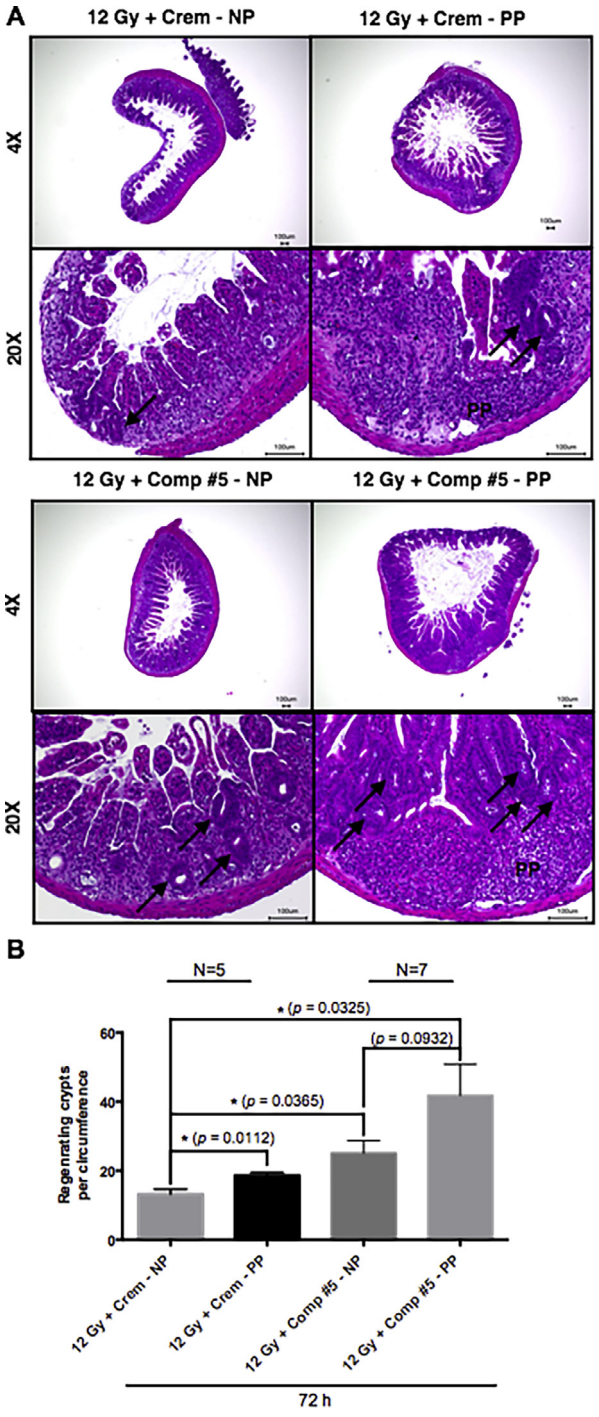

Fig. 4. Compound #5 increases the number of regenerating crypts in proximity to Peyer's patches. C3H mice received 12 Gy of total body irradiation. Control animals were sham-irradiated. Starting 24 h after irradiation 4 daily treatments of compound #5 (5 mg/kg) or Cremophor were administered subcutaneously. The mice were sacrificed, intestines were removed, fixed in formalin and embedded in paraffin blocks. Sections from these blocks were stained with H&E (A) and the regenerating crypts per circumference were counted (B). Compound #5 significantly increased the number of regenerating crypts per circumference in the 12 Gy + compound #5-treated PP-associated crypts versus the 12 Gy + Cremophor-treated non-patch-associated crypts (B).

Compound #5 increases the number of $CD45^+$ and $CD11b^{high}$ immune cells

In order to study the increase in immune cell subpopulations in more detail we used a panel of common markers and subjected PP cells to flow cytometry. $CD45^+$ cell numbers decreased 100-fold ($1.9 \times 10^5 \pm 4.5 \times 10^4$ to $1.8 \times 10^3 \pm 7.3 \times 10^2$; $p = 0.0023$, one-way ANOVA) after a single dose of 12 Gy. Treatment with compound #5 mitigated this effect of radiation ($1.8 \times 10^3 \pm 7.3 \times 10^2$ to $1.6 \times 10^4 \pm 1.3 \times 10^3$) but compared to non-irradiated controls the number of $CD45^+$ was still significantly reduced ($p = 0.0444$,

one-way ANOVA) 24 h after drug treatment and 48 h after irradiation (Fig. 3A).

Furthermore, in sham-irradiated animals treated with compound #5 increased the number of CD11b^{high} cells 14-fold ($2.2 \times 10^3 \pm 4.48 \times 10^2$ to $3.1 \times 10^4 \pm 1.2 \times 10^4$; $p = 0.0385$, Student's t-test) while the number of CD11c^{high} cells was not significantly altered (Fig. 3D and F). This increase in the percentage of CD11b^{high} cells resulted from an increase in the absolute number of CD11b^{highi} cells per Peyer's patch (Fig. 3B and E).

Compound #5 increases the number of regenerating PP-associated crypts

Regeneration of the epithelial lining of the intestines after radiation injury originates from surviving intestinal stem cells or reserve stem cells in the intestinal crypts. The gold standard used to assess effects of a drug modifying radiation responses of the intestines quantifies the number of regenerating crypts 96 h after irradiation [8]. When we analyzed cross sections of the small intestines of C3H mice 96 h after a single dose of 12 Gy and 72 h after treatment with Cremophor or compound #5 we detected a 2.6-fold higher number of regenerating crypts per circumference associated with PPs compared to the number of regenerating crypts in circumferences distant from PPs (61.33 ± 13.74 versus 23.50 ± 5.67; $p = 0.0362$, Student's t-test; Fig. 4).

To further investigate if the observed increase in the number of regenerating crypts was the result of an increased size of the intestinal stem cell pool, we next repeated the experiments using mice heterozygous for an Lgr5-EGFP knock-in gene in which intestinal stem cells are marked by EGFP expression. When we analyzed the small intestines of these animals treated with 12 Gy and 4 doses Cremophor or compound #5, we found a significant 2.1-fold increase in the percentage of Lgr5-EGFP + cells in animals treated with compound #5 (Fig. 5A, $p = 0.0299$, unpaired Student's t-test). Portions of these enteroid preparations were further cultured *in vitro* to test for functional intestinal stem cells, capable of forming budding crypts. Again, cells derived from compound #5-treated animals showed 1.8-fold increased numbers of budding crypts, 6 days after plating (Fig. 5B, $p = 0.0101$, unpaired Student's t-test). When we harvested and dissociated these enteroids into single-cell suspensions and re-analyzed them by flow cytometry we found that increased percentages of Lgr5-EGFP + intestinal stem cell populations in cells from compound #5-treated animals were maintained *in vitro* (Fig. 5C, $p = 0.0481$, unpaired Student's t-test).

Discussion

Recovery from GI ARS after radiation exposure to the abdomen depends on the successful restoration of the epithelial layer of the intestines, one of the more radiation-sensitive organs in the body. The functional units of the epithelial layer are organized hierarchically with intestinal stem cells at the base of the Lieberkuhn crypts. Transiently amplifying cells produce the differentiated cells of the layer that migrate like a conveyor belt to the tip of associated finger-like structures called villi, where the cells are shed off and die. After exposure to ionizing radiation the villi of the epithelial layer and crypt structures are rapidly lost and subsequently reconstituted from surviving intestinal stem cells that form regenerating crypts. Historically, cells in the +4 position of the Lieberkuhn crypts were believed to be the intestinal stem cells [9] but in recent years Lgr5$^+$ crypt base columnar (CBC) cells, wedged between Paneth cells, have been prospectively identified as the intestinal stem cell populations and they maintain tissue homeostasis under steady state conditions [10–13].

CBC cells are relatively radiosensitive [14–16] and after radiation injury, reserve stem cells in position +4 convert into Lgr5$^+$ cells and repopulate the niches of eliminated stem cells [17,18]. More recently, the ability to de-differentiate into Lgr5$^+$ intestinal stem cells was also attributed to all transiently amplifying cells as long as they have not left the crypt space [17] but it is less clear if this mechanism contributes to recovery after radiation injury. The number of regenerating crypts per circumference formed at 96 h after irradiation correlates with the survival of the animals [1]. Any drug that successfully mitigates radiation injury through an increase in regenerating crypts when given 24 h after irradiation will likely improve self-renewal of surviving intestinal stem cells or promote transdifferentiation of cells or dedifferentiation of transiently amplifying cells. However, while stem cell populations are restored and expanded, stem cell niches have to be recreated as well. Based on the increased radioresistance and the additional ring of cells found in these PP-associated crypts [2], one can speculate that GALT forms a larger stem cell niche that harbors more surviving intestinal stem cells and supports recovery after radia-

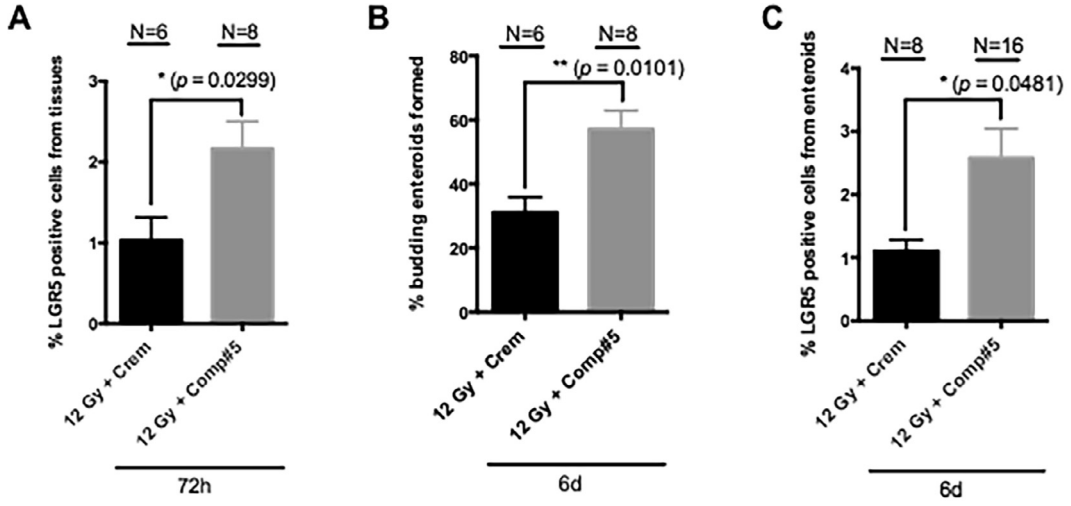

Fig. 5. Compound #5 increases the percentage of Lgr5-positive intestine stem cells. Lgr5-EGFP-IRES-creERT2 mice received 12 Gy of total body irradiation. Control animals were sham-irradiated. Starting 24 h after irradiation 4 daily treatments of Compound #5 (5 mg/kg) or Cremophor were administered subcutaneously. The mice were sacrificed, intestines were removed, crypts were isolated and the percentages of Lgr5-positive cells were analyzed by flow cytometry (A). The same number of crypts from each mouse was plated in 24-well plates embedded in matrigel and counted for budding enteroids 6 days after plating (B). Budding enteroids from Day 6 were dissociated to form a single-cell suspension and analyzed for the percentages of Lgr5-positive cells by flow cytometry (C).

tion injury. Evidence for immune cells providing niche components for intestinal stem cells was reported recently [19]. In this study we report that compound #5 mitigates GI-ARS by increasing the size and number of visible Peyer's patches and the number of regenerating crypts adjacent to the PPs. The increase in cellularity was most likely a result of immune cell recruitment to the PPs. The underlying mechanisms remain to be investigated. In summary our study suggests that GALT could be a promising target to mitigate GI ARS through the expansion of cell populations that provide niches for intestinal stem cells.

Conflict of interest statement

The authors declare no conflict of interest.

Acknowledgments

RD, JW, WM, and FP were supported by a grant from the National Institute of Allergies and Infectious Diseases (NIAID) (AI067769).

References

[1] Withers HR. Regeneration of intestinal mucosa after irradiation. Cancer 1971;28:75–81.
[2] Maunda KK, Moore JV. Radiobiology and stathmokinetics of intestinal crypts associated with patches of Peyer. Int J Radiat Biol Relat Stud Phys Chem Med 1987;51:255–64.
[3] Micewicz ED, Kim K, Iwamoto KS, Ratikan JA, Cheng G, Boxx GM, et al. 4-(Nitrophenylsulfonyl)piperazines mitigate radiation damage to multiple tissues. PLoS One 2017;12:e0181577.
[4] Booth C, Tudor G, Tudor J, Katz BP, MacVittie TJ. Acute gastrointestinal syndrome in high-dose irradiated mice. Health Phys 2012;103:383–99.
[5] Withers HR, Elkind MM. Microcolony survival assay for cells of mouse intestinal mucosa exposed to radiation. Int J Radiat Biol Relat Stud Phys Chem Med 1970;17:261–7.
[6] Grahn D, Hamilton KF. Genetic variation in the acute lethal response of four inbred mouse strains to whole body X-irradiation. Genetics 1957;42:189–98.
[7] Mason KA, Withers HR, McBride WH, Davis CA, Smathers JB. Comparison of the gastrointestinal syndrome after total-body or total-abdominal irradiation. Radiat Res 1989;117:480–8.
[8] Withers HR, Elkind MM. Radiosensitivity and fractionation response of crypt cells of mouse jejunum. Radiat Res 1969;38:598–613.
[9] Potten CS, Gandara R, Mahida YR, Loeffler M, Wright NA. The stem cells of small intestinal crypts: where are they? CellProlif 2009;42:731–50.
[10] Sato T, Vries RG, Snippert HJ, van de Wetering M, Barker N, Stange DE, et al. Single Lgr5 stem cells build crypt-villus structures in vitro without a mesenchymal niche. Nature 2009;459:262–5.
[11] Barker N, van Es JH, Kuipers J, Kujala P, van den Born M, Cozijnsen M, et al. Identification of stem cells in small intestine and colon by marker gene Lgr5. Nature 2007;449:1003–7.
[12] Barker N, van Es JH, Jaks V, Kasper M, Snippert H, Toftgard R, et al. Very long-term self-renewal of small intestine, colon, and hair follicles from cycling Lgr5 +ve stem cells. Cold Spring Harb Symp Quant Biol 2008;73:351–6.
[13] Clevers H. Lgr5 stem cell-based organoids in human disease. FASEB J 2017;31. 85.1–.1.
[14] Ishizuka S, Martin K, Booth C, Potten CS, de Murcia G, Burkle A, et al. Poly(ADP-ribose) polymerase-1 is a survival factor for radiation-exposed intestinal epithelial stem cells in vivo. Nucl Acids Res 2003;31:6198–205.
[15] Zhu Y, Huang YF, Kek C, Bulavin DV. Apoptosis differently affects lineage tracing of Lgr5 and Bmi1 intestinal stem cell populations. Cell Stem Cell 2013;12:298–303.
[16] Chang PY, Qu YQ, Wang J, Dong LH. The potential of mesenchymal stem cells in the management of radiation enteropathy. Cell Death Dis 2015;6:e1840.
[17] Tetteh PW, Basak O, Farin HF, Wiebrands K, Kretzschmar K, Begthel H, et al. Replacement of lost Lgr5-positive stem cells through plasticity of their enterocyte-lineage daughters. Cell Stem Cell 2016;18:203–13.
[18] Jones JC, Dempsey PJ. Enterocyte progenitors can dedifferentiate to replace lost Lgr5(+) intestinal stem cells revealing that many different progenitor populations can regain stemness. Stem Cell Investig 2016;3:61.
[19] Sehgal A, Donaldson DS, Pridans C, Sauter KA, Hume DA, Mabbott NA. The role of CSF1R-dependent macrophages in control of the intestinal stem-cell niche. Nat Commun 2018;9:1272.